Approximate Rate Constants for Nonideal Diffusion and Their Application in a Stochastic Model

Jeffrey W. Bullard

Materials and Construction Research Division, National Institute of Standards and Technology, Gaithersburg, Maryland 20899-8615

Received: September 7, 2006

Rate constants are presented for diffusion in dilute nonideal solutions with or without the presence of a spatially varying potential field. Expressions for the rate constants have been derived by earlier workers, and essentially the same derivation is reviewed and expanded in this paper to justify the expressions used for the rate constants. The diffusion rate constants are used in a random walker model to demonstrate how solution nonidealities can be captured accurately using this approach. Examples are presented of ideal solute diffusion as well as nonideal diffusion of nonelectrolytes and simple electrolytes in water. The use of the approach to simulate advection is described, and a possible strategy for extending the approach to more concentrated solutions is briefly discussed.

1. Introduction

The linear phenomenological rate law describing the material diffusion of a substance α is[1,2]

$$\mathbf{j}_\alpha = -L(\nabla\mu_\alpha - \mathbf{F}_\alpha) = -L\nabla\tilde{\mu}_\alpha \tag{1}$$

where $\mathbf{j}_\alpha$ is the net material flux in a laboratory reference frame, L is the Onsager coefficient for diffusion, μ_α is the chemical potential of the diffusing component, $\mathbf{F}_\alpha$ is any force per mole acting on the component, and $\tilde{\mu}_\alpha$ is the generalized chemical potential:

$$\tilde{\mu}_\alpha = \mu_\alpha + \psi_\alpha$$

in which ψ_α is a conservative potential field per mole of α, the spatial derivative of which is $-\mathbf{F}_\alpha$. Only the "direct" effect of diffusion is captured in eq 1 in the sense that off-diagonal coefficients representing cross-diffusion effects, thermal diffusion, Seebeck effects, etc. are neglected. When external forces are absent, material diffusion is frequently represented by Fick's first law

$$\mathbf{j}_\alpha = -D_\alpha\nabla c_\alpha \tag{2}$$

where c_α is the concentration (mol/L), and by comparison to eq 1, the diffusion coefficient is

$$D_\alpha = \left(\frac{\partial\mu_\alpha}{\partial c_\alpha}\right)_{P,T} L$$

Equations 1 and 2 provide expressions for the *net* flux at any point. Microscopically, mobile components at any point in an isotropic medium can have trajectories in all directions, not only the direction of the net flux. For example, in one-dimensional (1-D) diffusion, mobile components can have trajectories either in the same direction of the net flux (the *forward* direction) or in the opposite direction of the net flux (the *reverse direction*). By phrasing it this way, we suggest a loose analogy to chemical reactions. A chemical reaction proceeds in the forward direction, at an instantaneous rate that is prescribed by a specific rate constant, k_f, and the quantity of available reactants, to generate reaction products. As soon as products are present in the system, a reverse reaction is possible by which the products are transformed back to reactants, at a rate that is prescribed by a different rate constant, k_r, and the quantity of available products. Chemical equilibrium corresponds to a state in which the forward and reverse reactions occur at identical rates.

Transition state theory[3] provides a conceptual framework for describing separately the forward and reverse rates of chemical reactions. Not surprisingly, the same idea also can be applied to diffusion to determine the rate constants for the microscopic forward and reverse processes that macroscopically appear as a net flux down a gradient in potential.[4,5]

The difference in perspective between a phenomenological description of diffusion and a microscopic description has given rise to different approaches for simulating diffusion with computer models. Finite difference and finite element models take a phenomenological approach, by which a differential equation like eq 1 or eq 2 is numerically integrated on a mesh to determine the time-dependent concentration at each point. In contrast, random walker methods use a microscopic approach by which the random motion of individual particles is tracked.

This paper reviews how transition state theory can be used to derive approximate expressions for the forward and reverse rates of diffusion in nonideal solutions, relative to their absolute rates in a corresponding ideal solution. The possibility of a spatially varying potential field also is considered. The nonideal rate constants are then incorporated into a stochastic model of diffusion to simulate a number of different phenomena, including the ideal and nonideal diffusion of neutral species and electrolytes. Where possible, the stochastic simulation results will be compared to theoretical predictions to provide validation.

2. Diffusion Rate Constants

As already mentioned, most of the groundwork for deriving diffusion rate constants has been laid by others (see, for example, ref 4) for diffusion in nonideal solutions. The derivation is reviewed here primarily to provide explicit justification of the

10.1021/jp0658391 CCC: $37.00
Published on Web 02/24/2007

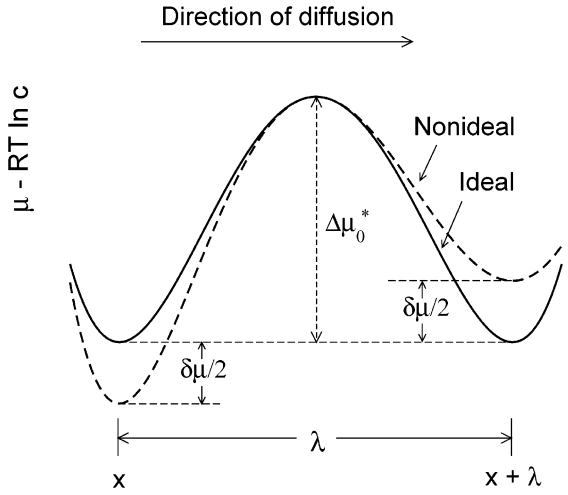

Figure 1. Schematic representation of the nonideal part of the chemical potential for diffusion in an ideal or nonideal solution. The horizontal dimension is the diffusion coordinate, and the vertical dimension is the nonconfigurational component of the chemical potential.

form of the rate constants used in this paper, and also because the approach is expanded to include the possibility of other forces acting on the system. We will consider the diffusion of a single component α in a solution. For simplicity of notation, the terms in this section will be understood to be associated with that component alone.

The elementary step in diffusion is assumed to be a "jump" between two positions, separated by a distance λ in physical space, each of which has a local minimum in free energy. The jump itself is assumed to involve passage through a state of higher free energy than either initial or final position. The process is illustrated schematically in Figure 1, which uses a scaled chemical potential to represent the energy states. In an ideal solution, the chemical potential μ of a component at any location is assumed to be $\mu^\circ + RT \ln c$, where μ° is the standard chemical potential of the component, c is its concentration, R is the gas constant, and T is the absolute temperature. The scaled chemical potential used in Figure 1 is defined as $\mu_0 \equiv \mu - RT \ln c$, i.e., the nonconfigurational part of the chemical potential. Therefore, in an ideal solution, the value of μ_0 is the same at every local minimum. This ideal situation is shown as the solid curve in the figure, for which both local minima are at the same height. The local configuration of solute and solvent corresponding to the maximum potential in the elementary step is called the *activated complex*. Although it has an exceedingly short lifetime, the activated complex is treated as an actual chemical species possessing well-defined chemical potential and other thermodynamic properties. Thus, in an ideal solution, the activation barrier for a component α, $\Delta\mu_0^*$ is the same in the forward and reverse directions.

The diffusion coefficient of the component α in an ideal solution is[4]

$$D_0 = \lambda^2 k_0 = \lambda^2 g e^{-\Delta\mu_0^*/RT} \tag{3}$$

where R is the gas constant, T is absolute temperature, and g is a jump frequency (units of s^{-1}) which usually is assumed to equal $k_B T/h$, with k_B being Boltzmann's constant and h being Planck's constant. In eq 3, k_0 is a specific rate constant for diffusion in the ideal solution, and has units of inverse time.

The chemical potential of activation may be divided into entropic and enthalpic contributions, i.e., $\Delta\mu_0^* = \Delta\bar{H}_0^* - T\Delta\bar{S}_0^*$, by which eq 3 may be rewritten as

$$k_0 = g' e^{-\Delta\bar{H}_0^*/RT} \tag{4}$$

where now $g' = g e^{\Delta\bar{S}_0^*/R}$, and $\Delta\bar{H}_0^*$ is the partial molar enthalpy of activation, which is essentially the same as the activation energy derived from the Arrhenius equation.

When a solution is nonideal, or when a potential field is present, the chemical potential of the component at any equilibrium position x is perturbed from its ideal value:

$$\begin{aligned}\tilde{\mu}(x) &= \mu^\circ + RT \ln a(x) + \psi(x) \\ &= \mu^\circ + RT \ln c(x) + RT \ln y(x) + \psi(x) \\ &= \mu_0(x) + RT \ln y(x) + \psi(x)\end{aligned} \tag{5}$$

where a is the chemical activity of the component, y is its molar activity coefficient, and ψ is the potential energy per mole of the component. Thus, in the nonideal case the difference in the chemical potential between adjacent sites is

$$\begin{aligned}\Delta\tilde{\mu}(x) &= (RT \ln y(x+\lambda) + \psi(x+\lambda)) - (RT \ln y(x) + \psi(x)) \\ &= RT\,\delta \ln y(x) + \delta\psi(x)\end{aligned} \tag{6}$$

This difference modifies the potential surface, shown as a dashed curve in Figure 1. Because the ideal surface is symmetric, it is assumed that the nonideal contribution to the potential difference is divided equally on either side of the barrier. This implies that the activation barrier in the forward direction is

$$\Delta\tilde{\mu}_f^* = \Delta\tilde{\mu}_0^* - \frac{RT}{2}\frac{\mathrm{d}\ln y}{\mathrm{d}c}\delta c(x) - \frac{\delta\psi(x)}{2} \tag{7}$$

where $\delta c(x) = c(x+\lambda) - c(x)$. In the reverse direction,

$$\Delta\tilde{\mu}_r^* = \Delta\tilde{\mu}_0^* + \frac{RT}{2}\frac{\mathrm{d}\ln y}{\mathrm{d}c}\delta c(x) + \frac{\delta\psi(x)}{2} \tag{8}$$

In both of these expressions, the activity coefficient is assumed to be a continuous function of the concentration. Given these results, we may now write down expressions for the forward and reverse rate constants relative to the ideal rate constant k_0. Following the form given in eq 3, the forward rate constant for component α jumping from x to $x + \lambda$ is written as

$$k_f = g e^{-\Delta\tilde{\mu}_f^*/RT} \tag{9}$$

Substituting eq 7 gives

$$\begin{aligned}k_f &= g e^{-\Delta\tilde{\mu}_0^*/RT} \exp\left(-\frac{1}{2}\frac{\mathrm{d}\ln y_\alpha}{\mathrm{d}c_\alpha}\delta c(x) - \frac{\delta\psi(x)}{2RT}\right) \\ &= k_0 e^{-\theta}\end{aligned} \tag{10}$$

where the last form comes from substituting the rate constant of component α in an ideal solution, eq 4, and

$$\theta = \frac{1}{2}\frac{\mathrm{d}\ln y_\alpha}{\mathrm{d}c_\alpha}\delta c(x) + \frac{\delta\psi(x)}{2RT} \tag{11}$$

The first term in θ expresses the departure from ideality due to the concentration dependence of the activity coefficients in nonideal solutions, and the second term indicates the effect of potential fields, whether externally applied or arising internally.

In the reverse direction, the specific rate constant for component α jumping from $x + \lambda$ to x is

$$k_r = k_0 e^{\theta} \tag{12}$$

Using the nonideal rate constants, the net material flux crossing the activation barrier at $x + \lambda/2$ can be found and compared to the phenomenological rate law in eq 1. The absolute number of moles of component α jumping across the activation barrier from x to $x + \lambda$ (i.e., the forward rate) will be denoted by $\dot{N}_f$ and is assumed equal to the forward rate constant multiplied by the number of moles at x,

$$\dot{N}_f = k_f(x)\, N(x)$$

or, in terms of the equivalent absolute flux j_f crossing the barrier in the forward direction (moles per unit area per unit time),

$$j_f(x+\lambda/2) = \lambda k_f(x)\, c(x)$$

Similarly, the absolute flux j_r crossing the barrier in the reverse direction is

$$j_r(x+\lambda/2) = \lambda k_r(x+\lambda)\, c(x+\lambda)$$

Therefore, the net flux j crossing the barrier in the forward direction is

$$\begin{aligned} j(x+\lambda/2) &\equiv j_f(x+\lambda/2) - j_r(x+\lambda/2) \\ &= \lambda k_f(x)\, c(x) - \lambda k_r(x+\lambda)\, c(x+\lambda) \end{aligned} \tag{13}$$

Substituting eqs 10 and 12 gives

$$\begin{aligned} j(x+\lambda/2) &= \lambda k_0 e^{-\theta} c(x) - \lambda k e^{\theta} c(x+\lambda) \\ &= \lambda k_0 (e^{-\theta} - e^{\theta})\, c(x) - \lambda k_{\alpha,0} e^{\theta} \delta c(x) \end{aligned} \tag{14}$$

where again $\delta c(x) = c(x+\lambda) - c(x)$. If $1 \gg \delta(\ln y)(x)$ and $2RT \gg \delta\psi(x)$, then $\theta \ll 1$ and the exponential terms in eq 14 can be expanded to first order in θ:

$$\begin{aligned} j(x+\lambda/2) &= -2\theta\lambda k_0 c(x) - (1+\theta)\lambda k_0 \delta c(x) \\ &= -2\theta\lambda k_0 c(x) - \lambda k_0 \delta c(x) \end{aligned} \tag{15}$$

where the second form comes from the assumption that $\theta \ll 1$. Substituting for θ gives

$$\begin{aligned} j(x+\lambda/2) &= -\lambda k_0 \left(c(x) \frac{\mathrm{d} \ln y}{\mathrm{d}c} \delta c(x) + \frac{c(x)}{RT} \delta\psi(x) + \delta c(x) \right) \\ &= \lambda k_0 \left(\left[1 + c(x) \frac{\mathrm{d} \ln y}{\mathrm{d}c} \right] \delta c(x) + \frac{c(x)}{RT} \delta\psi(x) \right) \\ &= \lambda^2 k_0 \left(\left[1 + \frac{\mathrm{d} \ln y}{\mathrm{d} \ln c} \right] \frac{\delta c(x)}{\lambda} + \frac{c(x)}{RT} \frac{\delta\psi(x)}{\lambda} \right) \end{aligned} \tag{16}$$

We can examine some of the properties of eq 16 to verify that it agrees with expectations of diffusion phenomena. If on a continuum scale c and ψ are continuous in x, then we may approximate

$$\frac{\delta c(x)}{\lambda} = \left. \frac{\mathrm{d}c}{\mathrm{d}x} \right|_{x+\lambda/2}$$

$$\frac{\delta\psi(x)}{\lambda} = \left. \frac{\mathrm{d}\psi}{\mathrm{d}x} \right|_{x+\lambda/2}$$

Then, because $\lambda^2 k_0 = D_0$ from eq 4, eq 16 can be written

$$j(x) = -D_0 \left(\left[1 + \frac{\mathrm{d} \ln y}{\mathrm{d} \ln c} \right] \left. \frac{\mathrm{d}c}{\mathrm{d}x} \right|_x + \frac{c(x)}{RT} \left. \frac{\mathrm{d}\psi}{\mathrm{d}x} \right|_x \right) \tag{17}$$

where a coordinate transformation $x + \lambda/2 \rightarrow x$ has been made for convenience.

If ψ is constant, then

$$j(x) = -D_0 \left(1 + \frac{\mathrm{d} \ln y}{\mathrm{d} \ln c} \right) \frac{\mathrm{d}c}{\mathrm{d}x} \tag{18}$$

This is identical to Fick's first law, eq 2, for which

$$D = D_0 \left(1 + \frac{\mathrm{d} \ln y}{\mathrm{d} \ln c} \right)$$

is the well-known expression for the diffusion coefficient in a nonideal solution. Second, in the presence of an external potential ψ, the generalized chemical potential[2] is given by eq 5. Differentiating eq 5 with respect to x gives

$$\begin{aligned} \frac{\mathrm{d}\tilde{\mu}}{\mathrm{d}x} &= RT \left(\frac{\mathrm{d} \ln y}{\mathrm{d}c} + \frac{\mathrm{d} \ln c}{\mathrm{d}c} \right) \frac{\mathrm{d}c}{\mathrm{d}x} + \frac{\mathrm{d}\psi}{\mathrm{d}x} \\ &= \frac{RT}{c} \left(1 + \frac{\mathrm{d} \ln y}{\mathrm{d} \ln c} \right) \frac{\mathrm{d}c}{\mathrm{d}x} + \frac{\mathrm{d}\psi}{\mathrm{d}x} \\ &= \frac{RT}{c} \left(\left[1 + \frac{\mathrm{d} \ln y}{\mathrm{d} \ln c} \right] \frac{\mathrm{d}c}{\mathrm{d}x} + \frac{c}{RT} \frac{\mathrm{d}\psi}{\mathrm{d}x} \right) \end{aligned} \tag{19}$$

The term inside parentheses is identical to the term inside parentheses in eq 17. Therefore, that equation can be written as

$$j = -\frac{cD_0}{RT} \frac{\mathrm{d}\tilde{\mu}}{\mathrm{d}x} \tag{20}$$

Equation 20 has the form of the linear phenomenological rate law given in eq 1.

In the next sections, we use the specific rate constants given by eqs 10 and 12 in a random walker model of diffusion. Examples are given of diffusion of a neutral component in ideal and nonideal solutions and of diffusion of a simple electrolyte.

3. Numerical Model

The stochastic model of diffusion used here is based on a random walker algorithm described by Karapiperis and Blankleider[6] for ideal solutions. A regular three-dimensional (3-D) cubic lattice is defined with site spacing λ, and each lattice site can be occupied by a number of random walkers, or cells, representing different mobile species. A parameter ξ is used to map the number of cells at a lattice site to an equivalent molar concentration. During a given computational cycle representing a time step τ, each cell in the system is allowed to take at most one step from its current location to one of its six nearest-neighbor sites chosen at random.

Karapiperis and Blankleider[6] have shown that to converge to the diffusion equation in the continuum limit, where $\lambda \rightarrow 0$ and $\tau \rightarrow 0$, the probability $p(i,j,\alpha)$ that a cell of solute species s_α is displaced from site i to a nearest-neighbor site j must be given by

$$p(i,j,\alpha) = \frac{D_{i,j,\alpha}\tau}{\lambda^2}$$

where $D_{i,j,\alpha}$ is the effective diffusion coefficient for transport of solute from site i to site j. For the purposes of the simulations, we now make the gross approximation that *the lattice spacing λ is equivalent to the jump distance λ* from the previous section.

Thus, in terms of specific rate constants, the probability is

$$p(i,j,\alpha) = k_{i,j,\alpha}\tau \tag{21}$$

Because each iteration of this diffusion algorithm corresponds to a time increment τ, the maximum time increment τ_{max} is fixed by requiring that the sum of the probabilities for each cell does not exceed 1. Thus, eq 21 can be used to estimate

$$\tau_{max} \leq \frac{1}{2n \max(k_{i,j,\alpha})} \tag{22}$$

where $\max(k_{i,j,\alpha})$ is the maximum expected specific rate constant, and n is the dimensionality of the problem ($n = 1$ for 1-D diffusion, etc.) so that $2n$ is the total number of nearest-neighbor lattice sites.

4, Results

4.1. Ideal Solution. Random walker models are known to closely approximate diffusion in ideal solutions, so the simulation of ideal diffusion is treated only briefly here. Consider an ideal neutral solute species A in a pure solvent. A small orthorhombic diffusion cell is modeled, having dimensions $x = 100$ μm and $y = z = 10$ μm. At time $t = 0$, the cell is filled with solvent, with the boundary conditions that $c_A = 15$ mmol/L at $x = 0$ μm and $c_A = 5$ mmol/L at $x = 100$ μm for all $t > 0$. Because the solution is ideal, the activity of the solute is equal to its concentration, and the diffusion coefficient is $D_{A,0}$ by definition. In this simulation, $D_{A,0} = 1000$ μm^2/s, which is the same order of magnitude as D_0 for most ions in water. Because the solution is assumed to be ideal, $\theta = 0$ in eqs 10 and 12

$$k_A \equiv k_{A,0} = D_{A,0}/\lambda^2 \tag{23}$$

This system has a straightforward analytical solution, which is obtained by solving the one-dimensional diffusion equation:

$$\frac{\partial c_A}{\partial t} = \frac{\partial}{\partial x}\left(D_A \frac{\partial c_A}{\partial x}\right) \tag{24}$$

$$c_A(x,t=0) = 0 \tag{24a}$$

$$c_A(0,t) = c_{A,0} \tag{24b}$$

$$c_A(L,t) = c_{A,L} \tag{24c}$$

The solution to eq 24 is

$$c_A(x,t) = \sum_{n=0}^{\infty} \frac{c_{A,L}\cos n\pi - c_{A,0}}{n} \sin\left(\frac{n\pi x}{L}\right) e^{-D_A n^2 \pi^2 t/L^2} \tag{25}$$

Figure 2 shows the predicted concentration profile in the simulated diffusion cell at different times when the mesh resolution $\lambda = 2$ μm and $\xi = 2.5 \times 10^{-5}$ mol/L. The symbols show the model prediction at each point and time, and the solid curves correspond to the analytical result, eq 25 with $L = 100$ μm, $c_{A,0} = 0.015$ mol/L, and $c_{A,0} = 0.005$ mol/L. The curves representing the analytical results all were obtained by truncating the sum at 10^4 terms.

Evidently, the model provides an excellent approximation to the standard diffusion equation at all times when $\lambda = 2$ μm. At the scale of Figure 2 the agreement appears to be nearly perfect. However, systematic deviations are evident in the region of the concentration minimum if the scale is magnified. Figure 3 shows a higher-resolution plot of the data at $t = 0.5$ s near the minimum

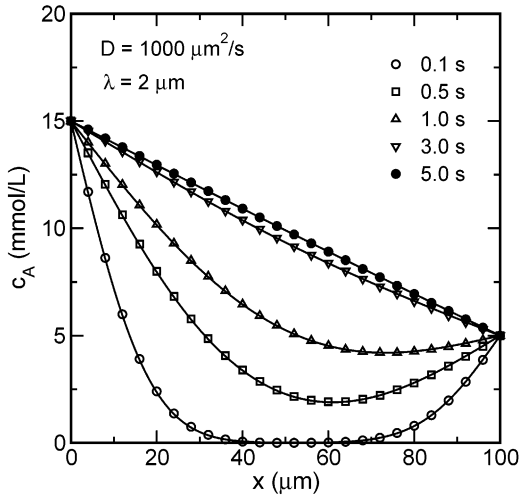

Figure 2. Comparison of non-steady-state concentration profiles predicted random walker model to analytical solutions of the 1-D diffusion equation (solid curves).

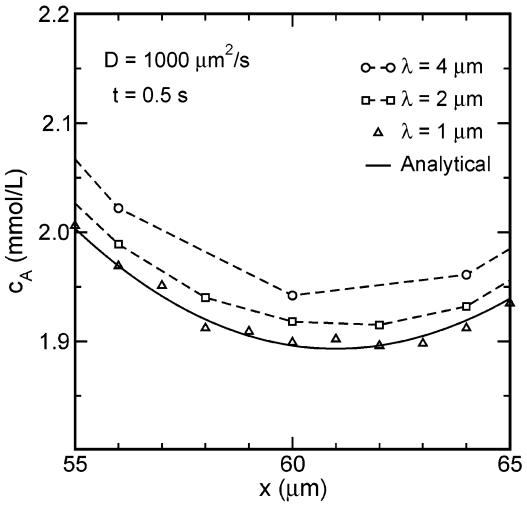

Figure 3. Dependence of predicted concentration profile at $t = 0.5$ s on the mesh resolution λ. The solid curve is the analytical solution to the diffusion equation at the same time. To distinguish the differences, only the region near the concentration minimum is shown.

in concentration. The simulated concentration profiles are shown for $\lambda = 1$, 2, and 4 μm. For $\lambda = 4$ μm, the simulation predicts concentrations that are too high everywhere, compared to the theoretical curve. The error is reduced significantly when the mesh resolution is refined to $\lambda = 2$ μm, although the predictions are still too high. When the resolution is further refined to 1 μm, the errors are quite small, even at the magnified scale of Figure 3. In addition, the predicted concentrations are no longer systematically too high at this resoluiton but appear to be scattered with a small amount of noise above and below the theoretical curve. The stochastic model therefore displays numerical convergence to the diffusion equation, at least down to a mesh resolution of 1 μm. At this level of mesh refinement, the small random errors introduced by the stochastic nature of the model are the main source of deviation from the theoretical result, rather than systematic error due to the resolution of the mesh.

This example was undertaken primarily because the diffusion equation has an analytic solution against which the simulations can be checked. In the remaining examples, an analytic solution of the diffusion equation is not readily available, and finite difference methods are used to numerically solve eq 24 for

comparison to the simulation results. In any event, the limiting case of diffusion in an ideal nonelectrolyte solution is useful for verifying the accuracy and convergence behavior of the stochastic model.

4.2. Diffusion in Nonideal Solutions. To model a solution of species A under nonideal conditions, we must assume a particular functional form for the dependence of the activity coefficient on concentration. Following the approximations made for nonelectrolytes,[7] the following power series approximation is used:

$$\ln y_A = 0.1 + 0.02c_A + 0.004{c_A}^2 \tag{26}$$

Three points are worth noting about this approximation. First, in solution thermodynamics it is customary to calculate activity coefficients on a *molal* basis instead of a concentration basis, because molality is independent of temperature. Thus, it is more common to express the molal activity coefficient γ_A as a function of molality of A. Nevertheless, one can convert all the terms and arrive at an approximation on a concentration basis. Second, eq 26 does not tend to zero as $c_A \rightarrow 0$, contrary to what might be expected. Instead, eq 26 can be thought of as being valid only over a range of concentrations significantly greater than 0. Finally, the dependence of $\ln y_A$ on concentration is assumed to be considerably stronger in eq 26 than what is observed experimentally for solutions like sucrose in water. A stronger dependence was assumed so that the consequences of departure from ideality can be more easily distinguished by the simulations.

Equation 26 was used to simulate a solution in a diffusion cell identical to that used in Figure 2, except that $c_A(0,t) = 5$ mol/L and $c_A(L,t) = 1$ mol/L, respectively. The rate constant was calculated using eq 10. For all the simulations, the approximation $\Delta x = \lambda$ was used. Therefore, for this example,

$$\begin{aligned}\theta &= \frac{\lambda}{2}\frac{\mathrm{d}\ln y_\alpha}{\mathrm{d}x} \\ &\approx \frac{\lambda}{2}\left(\frac{\ln y_\alpha(x+\lambda) - \ln y_\alpha(x)}{\lambda}\right) \\ &= \frac{1}{2}\ln\left(\frac{y_\alpha(j)}{y_\alpha(i)}\right)\end{aligned} \tag{27}$$

for a jump from site i to site j. Substituting into eq 10 gives

$$k_{i,j,\alpha} = k_\alpha\sqrt{\frac{y_\alpha(i)}{y_\alpha(j)}} \tag{28}$$

Figure 4 shows the simulated concentration profiles at 0.1 s (circles) and 1 s (squares). The solid curves are numerical solutions to eq 24 with

$$\begin{aligned}D_A &= D_{A,0}\left(1 + \frac{\mathrm{d}\ln y_A}{\mathrm{d}\ln c_A}\right) \\ &= D_{A,0}\left(1 + c_A\frac{\mathrm{d}\ln y_A}{\mathrm{d}c_A}\right) \\ &= 1000 + 20c_A + 8{c_A}^2\ (\mu\mathrm{m}^2/\mathrm{s})\end{aligned} \tag{29}$$

When the diffusion coefficient depends on concentration, analytical solutions to eq 24 are readily found only for infinite or semi-inifite slabs.[8] Therefore, the solid curves in Figure 4 were instead determined numerically using a simple finite difference model which uses a forward time centered space differencing scheme.[9] Finally, to appreciate the influence of nonideality, the predicted solutions to eq 24 assuming ideal behavior (i.e., $D_A \equiv D_{A,0}$) are shown as dashed lines.

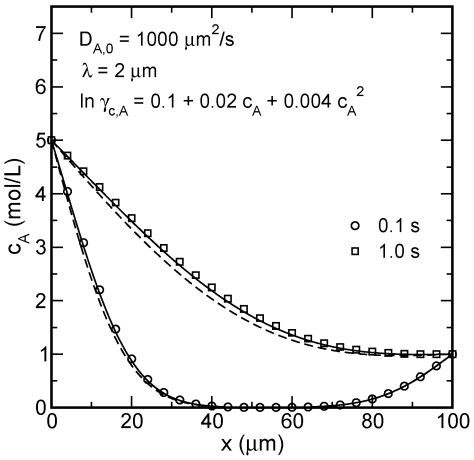

Figure 4. Diffusion in a single componenent nonelectrolyte solution under nonideal conditions. The open circle and square symbols are the simulation results at 0.1 and 1.0 s, respectively. The solid curves are the numerical solutions to the 1-D diffusion equation at the same times. The dashed curves are the analytical solutions to the 1-D diffusion equation under the assumption of ideality.

Figure 4 indicates that the differences between the ideal and nonideal solutions to the 1-D diffusion equation are fairly small, despite the fact that a strong dependence of the activity coefficients on concentration is assumed. The profile shapes are qualitatively the same, and the only quantitative difference is that the diffusion rate is slightly greater in the nonideal case, due to the positive value of the derivative in eq 29. Nevertheless, the stochastic simulation is sensitive enough to capture this small departure from ideality, which further indicates that the rate constant expressions are valid.

This example is intended to demonstrate the usefulness of eq 10 in capturing departures from ideality that are due only to the concentration dependence of the activity coefficients. However, at concentrations as great as those used here, another source of nonideality that is related to the increase in viscosity of the solution becomes quite important. This viscosity effect is not considered here but will be addressed in more detail in the Discussion.

4.3. Electrolyte Diffusion. The diffusion of an electrolyte that dissociates into ionic species presents at least two challenges that do not occur with diffusion of nonelectrolytes. The first challenge relates to the extent of dissociation. Strong electrolytes like NaCl have large equilibrium constants and dissociate completely in water up to fairly high concentrations, but weak electrolytes like $Ca(OH)_2$ do not. In addition, the ionic species that are present in solution may react to form ion complexes, and the relative amounts of these species are governed by thermodynamics. Thus in NaCl solutions at moderate concentrations, complete dissociation into equal numbers of Na^+ cations and Cl^- anions with no complexation is a good approximation, but $Ca(OH)_2$ solutions contain appreciable amounts not only of Ca^{2+} and OH^- but also of $CaOH^+$ and even of $Ca(OH)_2{}^0$.

The second challenge to simulating electrolyte diffusion is the constraint of preserving local charge neutrality. Anions typically have greater self-diffusion coefficients at infinite dilution than do cations. In a solution of NaCl, for example, the chlorine anions are capable of diffusing faster than the sodium cations. However, different rates of diffusion would set

up a charge separation. Thus in electrolytes the various ions are constrained to move at equal velocities despite any differences in their self-diffusion coefficients.[1,10] Therefore, ions in a diffusing electrolyte are subject to two forces. The first force is the usual (negative) gradient in chemical potential, and the second force is an electric field due to the motion of oppositely charged ions. Using a microscopic description, the more mobile ions will tend to diffuse at a greater rate than the less mobile ones, but this tendency sets up a local gradient in electrostatic potential in the solution. This second potential gradient will tend to increase the velocity of the less mobile ions and simultaneously decrease the velocity of the more mobile ions until they are diffusing at equal velocities.[10]

For electrolyte diffusion, therefore, the local specific rate constant is calculated according to eqs 10 and 11 with $\psi_\alpha \equiv -q_\alpha\phi$, where q_α is the electric charge (C/mol) and ϕ is the electrostatic potential, in J/C.

As a test of these ideas, the random walker model was applied to simulate diffusion in a solution of NaCl. The molar activity coefficients for both Na^+ and Cl^- were estimated using a modified Davies equation[11]

$$\ln y_\alpha = -\frac{Az_\alpha{}^2\sqrt{I}}{1 + a_\alpha B\sqrt{I}} + \frac{(0.2 - 4.17 \times 10^{-5}I)Az_\alpha{}^2 I}{\sqrt{1000}} \quad (30)$$

where I is the ionic strength of the solution,

$$I = \frac{1}{2}\sum_\beta z_\beta{}^2 c_\beta \quad (31)$$

with the sum taken over all the different types of ions and with z_β being the valence number of ion type β. In eq 30 A and B are temperature-dependent parameters given by

$$A = \frac{\sqrt{2}\mathscr{F}^2 e_o}{8\pi(\epsilon_w RT)^{3/2}} \quad (32)$$

$$B = \sqrt{\frac{2\mathscr{F}^2}{\epsilon_w RT}} \quad (33)$$

where $\mathscr{F}$ is Faraday's constant, e_o is the charge of an electron, and ϵ_w is the dielectric permittivity of water. Also in eq 30, the parameter a_α is comparable to an ionic radius, being equal to 3×10^{-10} m for Na^+ and 2×10^{-10} m for Cl^-. The modified Davies equation is a reasonably accurate estimation of activity coefficients of electrolyte species up to ionic strengths of about 0.2 mol/L.

Again supposing that $\Delta x = \lambda$, eq 11 becomes

$$\theta = \frac{1}{2}\ln\left(\frac{y_\alpha(j)}{y_\alpha(i)}\right) + \frac{-q_\alpha(\phi(j) - \phi(i))}{2RT}$$

for a jump of a single cell of species α from site i to nearest-neighbor site j. Because Na^+ and Cl^- both are univalent, $q_{Na^+} = \mathscr{F}$ and $q_{Cl^-} = -\mathscr{F}$. In addition, $D_{Na^+,0} = 1334$ $\mu m^2/s$ and $D_{Cl^-,0} = 2033$ $\mu m^2/s$ at 298 K.[12] Therefore, eqs 4 and 10 can be used to calculate the specific rate constants at 298 K:

$$k_{Na^+} = \frac{1334}{\lambda^2}\sqrt{\frac{y_{Na^+}(i)}{y_{Na^+}(j)}}e^{-\mathscr{F}(\phi(j)-\phi(i))/2RT} \quad (34)$$

$$k_{i,j,Cl^-} = \frac{2033}{\lambda^2}\sqrt{\frac{y_{Cl^-}(i)}{y_{Cl^-}(j)}}e^{\mathscr{F}(\phi(j)-\phi(i))/2RT} \quad (35)$$

The electrostatic potential at each lattice site i is estimated using a screened sum of charges over a neighborhood of the $M_{2\lambda}$ lattice sites separated from the given site by a distance of 2λ or less:

$$\phi(i) = \frac{\beta}{4\pi\epsilon_w}\sum_j^{M_{2\lambda}}\frac{\xi\lambda^3}{r(i,j)}\sum_k N_k q_k \quad (36)$$

where β is a dimensionless factor used to simulate the Coulombic screening of charge by water, which is set at 6×10^{-8} in this simulation, ϵ_w is the dielectric permittivity of water, and r_{ij} is the distance between lattice site i and j in units of λ. The conversion factor ξ again is set to 2×10^{-5} mol/L.

Figure 5 shows predicted concentration profiles for diffusion of NaCl in a 1-D diffusion cell like that used for the previous examples, except that the concentration of NaCl at the left boundary is fixed at 150 mmol/L and at the right boundary is fixed at 50 mmol/L. These concentrations approach the upper limit of applicability of the modified Davies equation, so this example should provide a fairly stringent test of the diffusion model. Concentration profiles at 0.2 and 1.0 s are shown in the figure, with the open symbols corresponding to Cl^- and the closed symbols corresponding to Na^+ concentrations. The upper and lower dashed curves surrounding each profile are the hypothetical concentration profiles of Cl^- and Na^+, respectively, if each behaved as an ideal neutral component.

It is evident from Figure 5 that the diffusion rate of Cl^- is decreased significantly, and that of Na^+ is increased modestly, due to the influence of the local electrostatic potential field that arises from transient charge separation. In fact, the simulated concentration profiles of Cl^- and Na^+ coincide quite closely at both of the time snapshots shown in Figure 5. In most regions the open symbol completely obscures the underlying filled symbol, and it is only near the minima in the profiles that appreciable differences are noticeable. Again, coincidence of the concentration profiles of both ions is expected if local charge neutrality is to be preserved.

The effective diffusion coefficient of NaCl in water is dependent on solute concentration and temperature. At 298 K, values have been measured experimentally with high accuracy over a range of concentrations.[1] Over the range of concentrations relevant to this example, a quadratic fit to these data is

$$D_{NaCl} \approx 1556.4 - 1.17842c_{NaCl} + 0.00381c_{NaCl}{}^2\ (\mu m^2/s) \quad (37)$$

Numerical solution of eq 24 using a finite difference approach—with eq 37 substituted for D—thus provides "experimental" concentration profiles to which the stochastic model predictions can be compared.

Figure 6 shows such a comparison for time snapshots of predicted concentration at 0.2 s, 0.5, 1.0, and 2.0 s. Once again, the open and closed symbols correspond to predicted concentrations of Cl^- and Na^+ respectively. The solid curves correspond to the numerical solution of eq 24 using eq 37 for D_{NaCl}.

The figure indicates that the stochastic model provides good quantitative agreement with the profiles expected from experimental measurements of D_{NaCl}. In fact, the agreement at all times is at least as good as for nonideal but neutral solute diffusion shown in Figure 4.

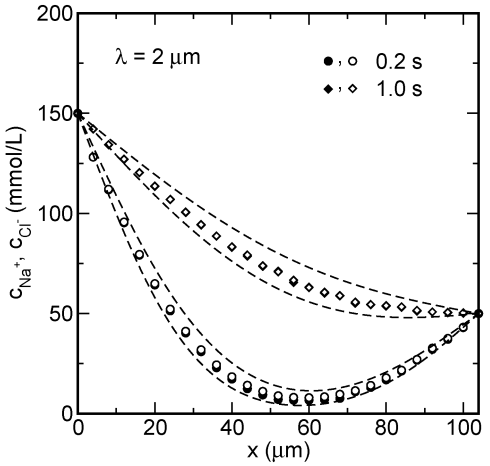

Figure 5. Diffusion of NaCl. The open symbols indicate the concentration profiles of Cl^- and the closed symbols indicate the concentration profiles of Na^+. The upper and lower dashed curves surrounding each profile correspond to the ideal concentration profiles of Cl^- and Na^+, respectively, based only on their self-diffusion coefficients at infinite dilution.

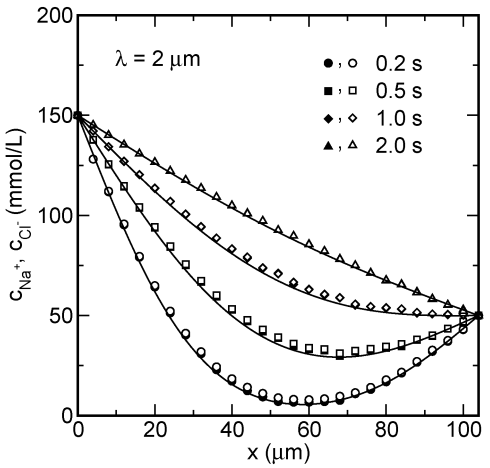

Figure 6. Comparison of NaCl concentration profiles predicted by the stochastic model (symbols) to those predicted using experimentally observed effective diffusion coefficients for NaCl in ref 1 (solid curves). The open symbols indicate the concentration profiles of Cl^- and the closed symbols indicate the concentration profiles of Na^+.

This rather simple stochastic model appears to capture some basic electrolyte diffusion phenomena quite well. However, a somewhat subtle problem with the model exists as the system approaches steady state. Specifically, the stochastic model used here predicts a linear concentration profile for both Na^+ and Cl^-. When the model obtains this steady state, the electrostatic potential is decreased to zero everywhere, and therefore the fluxes of Na^+ and Cl^- can differ while still maintaining charge neutrality at each node. That is, the stochastic model predicts that the effective diffusion coefficients of Na^+ and Cl^- return to their infinite-dilution values as a steady state is approached. In reality, a system like that simulated here will exhibit a nonlinear concentration profile at steady state, along with a well-defined liquid junction potential that depends only on the difference in end point concentrations. This potential exactly counteracts the tendencies of the different ions to diffuse at different rates and therefore not only preserves charge neutrality but also keeps the velocities of the different ions equal.

The stochastic model used here is unable to capture the phenomenon of a liquid junction potential, but that seems to be a limitation of the type of model used rather than a limitation of the expressions for the rate constants. Continuum approaches to electrolyte diffusion, which numerically solve the Nernst−Planck and Poisson equations, also fail to capture this effect unless an a priori balance of charge flux is used to enforce charge neutrality.[13]

5. Discussion

The transition state approach used by Eyring and others[4] to derive rate constants for diffusion has been criticized as being oversimplified. The principal objection to the approach is that it seems to assume a quasi-crystalline structure of the liquid so that the idea of discrete jumps between equilibrium sites becomes meaningful. Furthermore, the accuracy with which the theory predicts *absolute* diffusion rates in water is known to be poor, a fact that was acknowledged even by Eyring and co-workers.[4] Nevertheless, the basic ideas of transition state theory—distinguishing specific rate constants for forward and reverse processes, the existence of an activation barrier, etc.—are extremely helpful from a qualitative viewpoint. Provided that one is not trying to predict absolute values of the rate constants, the approach is useful for approximating *relative* influences of temperature and nonideality on diffusion rates, the *absolute* values of which are assumed known under ideal conditions.

The agreement between the transition state approach and the linear phenomenological rate laws, which was demonstrated in eqs 18 and 19, occurs only when θ in eq 11 is much smaller than 1. This low value allows the expansion of the exponential factor to first order, upon which the linear rate law is recovered. In the overwhelming majority of practical situations, θ will indeed be much smaller than 1, but it is still interesting to consider the nature of the disagreement between the two approaches when θ is not small. The linear law embodied in eq 1 has been experimentally validated over a wide range of conditions but, nevertheless, is recognized as a "special case" that may need to be extended to account for nonlinearities under certain circumstances.[14] Focusing attention on the potential field term in eq 11, if one considers $\nabla\psi$ to be a body force operating per unit mass, then for diffusion $\lambda\nabla\psi$ can only be comparable to RT if $\nabla\psi$ is about 10^{13} times greater than the acceleration due to gravity on the Earth's surface. This would seem to qualify as a situation that is extremely far from equilibrium, even on a microscopic scale, and we may begin to be suspicious of the applicability of the linear rate law. On the other hand, the transition state approach involves several assumptions that would make its validity at least as dubious under such conditions. For example, the chemical potential of the activated complex is assumed to be the same under ideal and nonideal conditions (see Figure 1). But there is no reason to expect that this assumption holds under extremely large driving forces and, if this assumption is invalid, it is difficult to assess the relative changes in the forward and reverse rate constants under nonideal conditions. Therefore, because the assumptions of both approaches become questionable under such extreme conditions, at this point it may be advisable to simply confine attention to the broad range of conditions under which they agree with each other.

Accepting the restriction to moderate driving forces, and knowing that nonidealities affect the rates of diffusion at any temperature, we may also ask whether the activation energy is affected too. Departures from ideality, due to either the concentration dependence of the activity coefficients or the effect of potential fields, are embodied in eqs 10 and 11. The former effect contributes a term to the chemical potential, eq 5, that is

linear in temperature, and that linearity in T is cancelled when the activation barrier is divided by RT in the argument of the exponential term in the rate constant. Therefore, nonideality due only to the concentration dependence of the activity coefficients does not contribute significantly to the temperature dependence of the rate constant. [There is in fact a modest temperature effect because the activity coefficients themselves change with temperature.]

In contrast to this chemical interaction effect, the influence of a potential field contributes an additive term to the chemical potential that is independent of temperature. Therefore, a $1/T$ dependence carries through with the potential in eqs 10−12. Assuming no chemical interactions, i.e., $y_\alpha \equiv 1$, then substituting eq 4 into eq 10 and rewriting gives

$$k_{\alpha,f} = g' \exp\left[\frac{-\left(\Delta^{\bar{H}*}_{\alpha,0} + \frac{\lambda}{2}\frac{d\psi_\alpha}{dx}\right)}{RT}\right] \tag{38}$$

Thus, a spatially varying potential field could conceivably modify the activation energy for diffusion. However, as discussed earlier, any such effect would be observable only under such large potential gradients that the overall approach becomes questionable. Therefore, in any practical situation, potential gradients also should have a negligible influence on the activation energy.

An important influence on diffusion rates, which has not been considered directly in this treatment, is the viscosity of the liquid. Diffusion and viscous flow in liquids are closely related phenomena. Chandra and Bagchi[15] have shown for electrolytes how the classical descriptions of these phenomena can be unified by a microscopic theory based on mode coupling. Both diffusion and viscous flow are rate processes, and the activated complex in both cases corresponds to a saddle point in potential energy that arises as molecules slide past one another. Thus, the activation energies of both processes are the same, as shown earlier by Li and Chang.[16]

The Stokes−Einstein law provides a relation between the diffusion coefficient of solute in a dilute solution and the viscosity η of the solvent:

$$D \propto \frac{1}{T\eta} \tag{39}$$

Over a modest range of temperatures, the $1/T$ factor in this equation is much weaker than the exponential temperature dependence of D and η, so both processes have approximately the same temperature dependence. As a result, in ideal or dilute solutions, the effect of viscosity on diffusion indicated in eq 39 is accommodated in the temperature dependence of D_0 given in eq 4. In addition, the viscosity of dilute solutions is approximated by the Einstein relation,[17]

$$\eta = \eta_0(1 + \alpha\phi)$$

where α is a system-dependent constant and ϕ is the volume fraction of solute and η_0 is the viscosity of the pure solvent. This means that the viscosity of a very dilute solution, for which $\phi \ll 0.4$, is not appreciably different from that of the solvent. Therefore, the rate constants provided in eqs 10 and 12 should be a good approximation when simulating diffusion either in ideal or in dilute nonideal systems.

The situation is more complicated at higher concentrations[15] where the viscosity of the solution differs appreciably from that of the solvent at the same temperature. In concentrated systems, the diffusion coefficients, and therefore the specific rate constants, will still vary inversely with the solution viscosity.[1,10] Thus, the forward and reverse rate constants for diffusion have a composition dependence that has not been considered explicitly in this paper. However, if the viscosity of a solution at a particular average composition were known relative to the pure solvent, then one could estimate the pertinent diffusion coefficient relative to its value in an ideal solution according to eq 39. With this estimate in hand, the diffusion coefficient could then be related to the specific rate constants using eqs 4, 10, and 12.

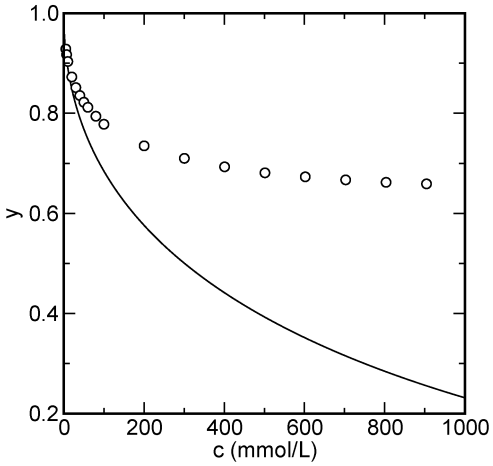

Figure 7. Molar activity coefficients for NaCl approximated by the modified Davies equation (solid curve) compared to the experimentally measured values (open circles) as a function of concentration. Experimental data taken from refs 1 and 10.

In the example of diffusion of NaCl given in the previous section, a modified Davies equation was used to approximate the activity coefficients. With this approximation, the activity coefficients decrease more severely with concentration than they do in real solutions, as shown in Figure 7. The discrepancy at higher concentrations means that the approximation will exaggerate the magnitude of $d(\ln y)/d(\ln c)$, thereby underestimating the effective diffusion coefficient of each ion. Therefore, in that particular example, the error involved in the approximation of activity coefficients fortuitously helps to compensate for the error in neglecting the increasing viscosity at higher concentrations. At the low concentrations used in this example, neither of these offsetting errors is extremely large, but one should be aware of these issues when modeling at higher concentrations: expending the effort to account for solution viscosity might produce seemingly poorer predictions if the Davies equation is used for the activity coefficients.

With regard to high-concentration effects, there is no doubt that continuum approaches exist that can provide more accurate results over a wider range of concentrations, both for nonelectrolytes and especially for electrolyte diffusion.[18,19] However, an advantage of the approach used here is that it is well-suited for incorporation into stochastic numerical models, as shown by the examples in the previous section. For certain types of problems, simulation by a stochastic method may be preferable to continuum simulations because stochastic methods can be relatively easy to implement and they often avoid numerical stability issues that can arise in some continuum approaches. Furthermore, in reaction-diffusion problems, a stochastic approach could enable the investigation of spatial correlations among reacting species, which can result when the rates of diffusion and reaction are comparable. Continuum approaches to these problems are based on mean-field approximations for

concentration and implicitly assume that such correlations are smoothed out over the length scale of interest.[6]

In closing, it may be noted that the rate constant approach described here can be expanded naturally to include advection phenomena. As a simple example, in the limiting regime of ideal diffusion, $k_{\alpha,f} = k_{\alpha,r}$. A uniform velocity v_α of a particular mobile species in the x direction, in a reference frame that moves with the solvent, can be simulated by biasing the rate constants in that direction such that $k_{\alpha,f} - k_{\alpha,r} = v_\alpha/\lambda$. Referring to eqs 10−12, it is easy to show that

$$\frac{d\psi_\alpha}{dx} = -\frac{RTv_\alpha}{k_{\alpha,0}\lambda^2} \tag{40}$$

In other words, this velocity of species α will be simulated by the random walker algorithm if one assigns a potential energy to each lattice site (x, y, z) given by

$$\psi_\alpha(x,y,z) = -\left(\frac{RTv_\alpha}{k_{\alpha,0}\lambda^2}\right)x \tag{41}$$

to within an additive constant. This idea could be further expanded to model segregation of species with different molecular masses under the influence of a constant body force.

6. Summary

Specific rate constants for diffusion in nonideal solutions, with or without the presence of a potential field, have been derived using ideas from transition state theory. The approach is effectively the same as that used by the original proponents of transition state theory over 60 years ago, and the results are in agreement with that earlier work. When these rate constants are incorporated into a random walker model, the influences of solution nonideality can be simulated accurately both for nonelectrolytes and for simple electrolytes at dilute concentrations. The accuracy of the model to higher concentrations, greater than 0.1 mol/L, is dependent on the ability to estimate viscosity as a function of composition.

Acknowledgment. The author and this paper both have benefitted greatly from numerous and insightful discussions with Ken Snyder at the National Institute of Standards and Technology.

References and Notes

(1) Harned, H. S.; Owen, B. B. *The Physical Chemistry of Electrolytic Solutions*, 3rd ed.; Reinhold Publishing: New York, 1958.
(2) de Groot, S. R.; Mazur, P. *Non-Equilibrium Thermodynamics*; Dover Publications: New York, 1984.
(3) Eyring, H. *J. Chem. Phys.* **1935**, *3* (2), 107.
(4) Glasstone, S.; Laidler, K. J.; Eyring, H. *The Theory of Rate Processes*; McGraw-Hill: New York, 1941.
(5) Hill, T. L. *Proc. Nat. Acad. Sci. U.S.A.* **1976**, *73* (3), 679−683.
(6) Karapiperis, T.; Blankleider, B. *Physica D* **1994**, *78*, 30−64.
(7) Noggle, J. H. *Physical Chemistry*; Little, Brown, and Co.: Boston, MA, 1985.
(8) Crank, J. *The Mathematics of Diffusion*; Oxford University Press: Oxford, England, 1956.
(9) Press, W. H.; Teukolsky, S. A.; Vetterling, W. T.; Flannery, B. P. *Numerical Recipes in C*, 2nd ed.; Cambridge University Press: London, 1997.
(10) Robinson, R. A.; Stokes, R. H. *Electrolyte Solutions*, 2nd ed.; Dover Publications: New York, 1959.
(11) Samson, E.; Marchand, J.; Beaudoin, J. J. *Cem. Concr. Res.* **2000**, *30*, 1895−1902.
(12) Mills, R.; Lobo, V. M. M. *Self-Diffusion in Electrolyte Solutions*; Elsevier: Amsterdam, 1989.
(13) Riveros, O. J.; Croxton, T. L.; Armstrong, W. M. *J. Theor. Biol.* **1989**, *140*, 221−230.
(14) Compte, A.; Jou, D. *J. Phys. A* **1996**, *29*, 4321−4329.
(15) Chandra, A.; Bagchi, B. *J. Phys. Chem. B* **2000**, *104*, 9067−9080.
(16) Li, J. C. M.; Chang, P. *J. Chem. Phys.* **1955**, *23*, 518.
(17) Einstein, A. *Ann. Phys.* **1906**, *19*, 289−305.
(18) Snyder, K. A. *Concr. Sci. Eng.* **2001**, *3*, 216−224.
(19) Samson, E.; Marchand, J.; Snyder, K. A.; Beaudoin, J. J. *Cem. Concr. Res.* **2005**, *35* (1), 141−153.